Formation of electric-field domains in GaAs/$Al_xGa_{1-x}As$ quantum cascade laser structures

S. L. Lu, L. Schrottke, S. W. Teitsworth,* R. Hey, and H. T. Grahn†
Paul-Drude-Institut für Festkörperelektronik, Hausvogteiplatz 5-7, 10117 Berlin, Germany
(Received 30 September 2005; revised manuscript received 28 November 2005; published 13 January 2006)

The current-voltage (*I-V*) characteristics of GaAs/$Al_xGa_{1-x}As$ quantum cascade laser structures (QCLSs) are found to exhibit current plateaus with discontinuities for voltages below threshold. The number of current discontinuities is correlated with the number of periods of the QCLS, suggesting the formation of electric-field domains that span the entire structure. A self-consistent calculation of the conduction band profile and corresponding electronic wave functions shows that the low-field domain is related to resonant tunneling between the ground state g in the active region and the lowest energy state in the adjacent, downstream injector i_1. For $x=0.33$ ($x=0.45$), the high-field domain is formed for resonant tunneling between g and the first (second) excited state i_2 (i_3) in the injector region. A comparison of the experimental data with the calculated conduction band profile shows that a significant field inhomogeneity within each period shifts the voltage range, for which the resonance condition is fulfilled, to much lower voltages than expected for a homogeneous field distribution.

DOI: 10.1103/PhysRevB.73.033311 PACS number(s): 73.21.Cd, 73.63.Hs

I. INTRODUCTION

Population inversion in quantum cascade laser structures (QCLSs) is achieved by resonant coupling of the injector state of a given period with the upper laser level of the same period so that electrons tunnel resonantly into the active region.[1] As a result, a negative differential conductance (NDC) regime is expected above threshold. Recent theoretical[2] and experimental investigations[3] on the transport properties of GaAs/$Al_xGa_{1-x}As$ QCLSs have shown that the NDC due to the resonant coupling between the injector and upper laser level appears only for the investigated sample with $x=0.45$ and not with $x=0.33$. However, the experiments revealed a bistable NDC for both Al contents at lower field strengths. In addition, a recent theoretical investigation on the influence of the doping density on the performance of GaAs/$Al_xGa_{1-x}As$ QCLs by Jovanović *et al.*[4] demonstrated that in the high pumping-current regime a V-shaped electric-field inhomogeneity referred to as local field domains is present in each period, preventing resonant subband level alignment.

For electric-field strengths well below threshold, plateau-like structures in the current-voltage (*I-V*) characteristics of QCLSs have been reported,[5,6] which are similar to *I-V* characteristics observed in weakly coupled semiconductor superlattices (SLs) under electric-field-domain formation. In the latter case, it is well known that the formation of such domains is a consequence of NDC originating from resonant tunneling between different subbands in adjacent wells.[7] A single low-field and a single high-field domain span the entire SL, and they are separated by a charge accumulation layer, which allows for the change of the electric-field strength across the domain boundary. In the case of QCLSs, this global domain formation occurs at voltages far below the lasing threshold so that tunneling resonances at field strengths much smaller than the threshold field strength may be responsible for this global field inhomogeneity. In QCLSs, a local field-domain formation within each period as discussed in Ref. 4 may appear in addition to the global domain formation of the type observed for the SL structures. These local field domains are induced by the separation of the electrons from the ionized donors. A better understanding of the role of such local field domains caused by the interplay of a high doping level with the complex subband structure in QCLSs is necessary for a further improvement of the operation characteristics of QCLs. Furthermore, it may help to explain the dependence of the lasing properties on the injector doping density[4,8] and improve the insight into the correlation between population inversion and threshold current density of QCLs.[9]

In this paper, we investigate the formation of global electric-field domains in GaAs/$Al_xGa_{1-x}As$ QCLSs, which is observed through the appearance of plateaulike structures in the *I-V* characteristics. We calculate self-consistently the potential profile and the corresponding wave functions on the basis of a scattering-rate model for an infinitely long structure that assumes periodic boundary conditions and that is similar to models published by Donovan *et al.*[10] and Jovanović *et al.*[4] This permits the determination of the voltage for which electrons resonantly tunnel from the ground state g in the active region into the three lowest energy states in the downstream injector i_1, i_2, and i_3. The voltage, at which resonant tunneling into these states is predicted to occur, is compared to the voltage range of the plateaus in the measured *I-V* characteristics.

II. EXPERIMENT

The investigated samples were grown by molecular-beam epitaxy on n^+-GaAs (100) substrates. Sample A is a GaAs/$Al_{0.33}Ga_{0.67}As$ QCLS based on the design by Sirtori *et al.*[11] with 30 periods. Starting with the injection barrier, the layer sequence of one period is **5.8**, 1.5, **2.0**, 4.9, **1.7**, 4.0, **3.4**, 3.2, **2.0**, 2.8, **2.3**, 2.3, **2.5**, 2.3, **2.5**, and 2.1 nm (bold numbers indicate barriers and underlined ones are the doped layers). Sample B is a GaAs/$Al_{0.45}Ga_{0.55}As$ QCLS based on the design of Page *et al.*[12] with 36 periods. The layer sequence for this sample is **4.6**, 1.9, **1.1**, 5.4, **1.1**, 4.8, **2.8**, 3.4,

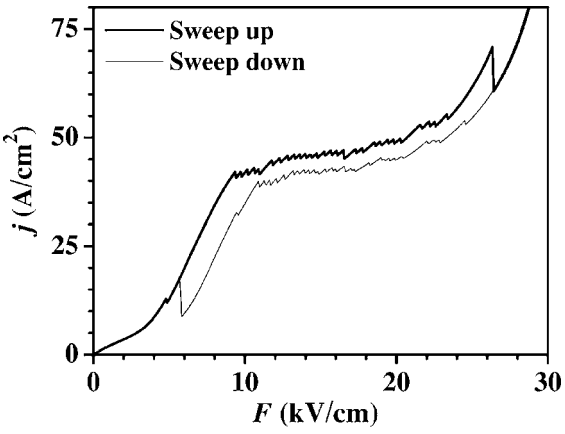

FIG. 1. *I-V* characteristics of sample A for a sweep up (thick line) and sweep down (thin line) recorded at 6 K. The average field has been calculated from the applied voltage divided by the thickness of the cascade structure without the cladding layers (1.36 μm).

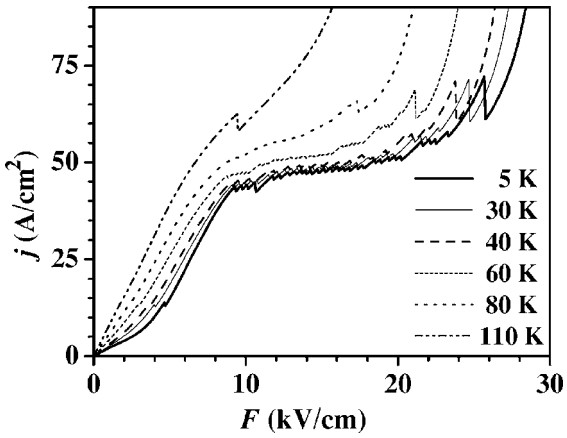

FIG. 2. *I-V* characteristics of sample A for different temperatures as indicated.

1.7, 3.0, **1.8**, 2.8, **2.0**, 3.0, **2.6**, and 3.0 nm. For both samples, the QCLS is sandwiched between two pairs of Si-doped GaAs layers (4 μm with 4×10^{16} cm^{-3} and 1 μm with 4×10^{18} cm^{-3}) on the substrate and on the top side.

For the *I-V* measurement, the samples were processed into rectangular mesas with an area of 45×170 μm^2 and 19×100 μm^2 for samples A and B, respectively. The *I-V* characteristics were recorded using a voltage source (Hewlett-Packard, model 3245A) and a digital multimeter (Hewlett-Packard, model 3458A) in a two-terminal configuration. During the measurements, the samples were cooled on a cold finger of a He flow cryostat.

III. *I-V* CHARACTERISTICS

Figure 1 shows a typical *I-V* characteristic of sample A at 6 K for different sweep directions. Because the electric-field distribution is inhomogeneous, we can only determine an average electric field, which is calculated from the applied voltage and the thickness of the cascade structure excluding the doped cladding layers. This average electric field is used in the figures as the abscissa. The *I-V* characteristic in Fig. 1 exhibits a plateaulike region between 9 and 24 kV/cm with 28 discontinuities. The number of jumps (28) in the current density is almost equal to the number of periods of the cascade structure of sample A, which is 30. For the case of electric-field-domain formation in doped, weakly coupled SLs, each discontinuity corresponds to the motion of the domain boundary by one period. In addition, the *I-V* characteristic displays a clear hysteresis between sweep-up and sweep-down directions, but the number of discontinuities is the same. As in doped, weakly coupled SLs, the hysteresis is caused by multiple possible locations of the domain boundary for a fixed applied voltage.[7] At about 27 kV/cm for the up-sweep direction and 6 kV/cm for the down-sweep direction, a very pronounced single NDC peak appears, which is similar to the one observed in undoped quantum cascade (QC) structures.[3] These field strengths are clearly below the theoretical threshold field strength of 48 kV/cm as given in Ref. 11. Note that the measured threshold field strengths are usually considerably larger. Figure 2 shows *I-V* characteristics of sample A for different temperatures between 5 and 110 K. With increasing temperature, the amplitude of the discontinuities gradually decreases. Above 80 K, the small discontinuities disappear, while the pronounced single NDC peak remains clearly visible even at 110 K. At the same time, the plateau shifts to lower voltages spanning a decreasing voltage range with increasing temperature. The shift to lower voltages and the decrease of the amplitude of the discontinuities with increasing temperature in the *I-V* characteristics may be qualitatively explained by an enhancement of electron-phonon scattering with increasing temperature. The origin of the single pronounced NDC peak is still unresolved. One possibility is an effect of the transition region between the contact layer and the first period of the cascade structure, which acts as a disturbance on the periodicity of the whole cascade structure. A similar behavior is observed for sample B as shown in Fig. 3. The inset displays an enlarged part of the *I-V* characteristic for lower voltages.

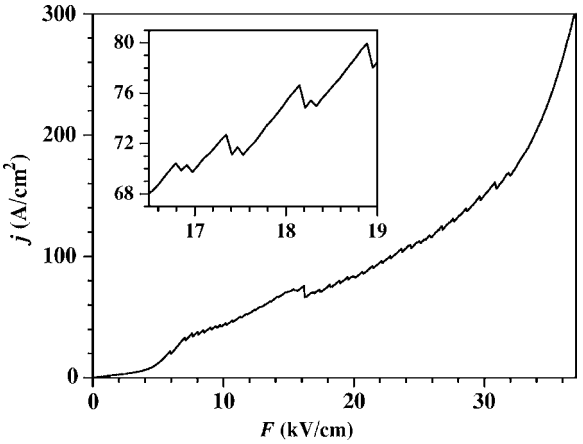

FIG. 3. *I-V* characteristics of sample B at 6 K. The average field has been calculated from the applied voltage divided by the thickness of the cascade structure without the cladding layers (1.62 μm). Inset: Enlarged part of the *I-V* characteristics for the lower field range.

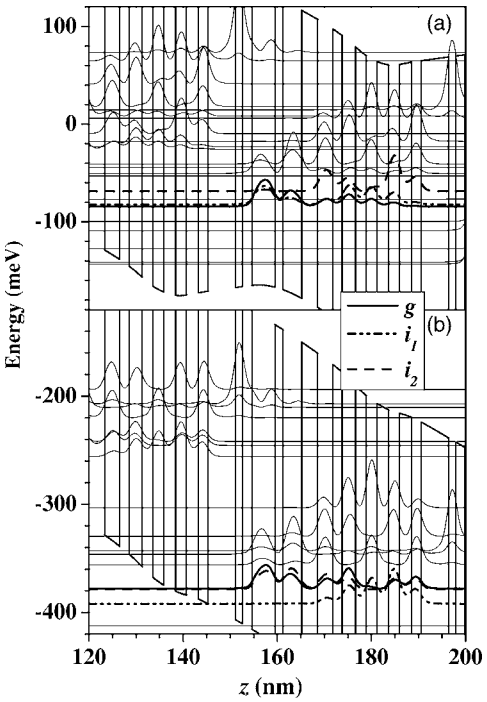

FIG. 4. Calculated conduction band profile and electron probability density at two average electric field strengths, (a) $F_1=13$ kV/cm and (b) and $F_2=28$ kV/cm, for sample A. g denotes the ground state in the active region and i_1 and i_2 the lowest two states of the adjacent, downstream injector.

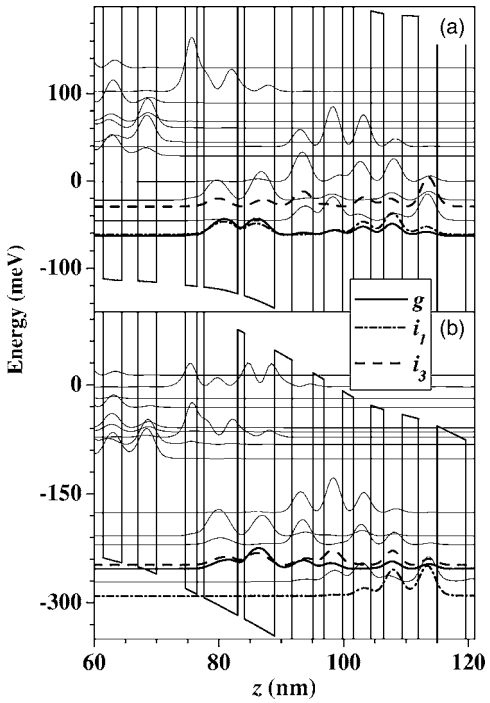

FIG. 5. Calculated conduction band profile and electron probability density at two average electric field strengths, (a) $F_1=20$ kV/cm and (b) and $F_2=42$ kV/cm, for sample B. g denotes the ground state in the active region and i_1 and i_3 the lowest two states of the adjacent, downstream injector.

Again, there is a correlation between the number of discontinuities (35) with the number of periods (36) indicating the formation of global electric-field domains.

IV. DISCUSSION

In conventional SLs, sequential resonant tunneling usually takes place between different subbands in adjacent wells. For a low-field domain caused by resonant tunneling between two energy levels E_0 and E_1 and a high-field domain caused by resonant tunneling between two energy levels E_0 and E_2, the difference in the voltage drops per period between the high-field and the low-field domains can be calculated according to[7,13]

$$\Delta V = (E_2 - E_0 - [E_1 - E_0])/e = (E_2 - E_1)/e, \qquad (1)$$

where e denotes the elementary charge. We have neglected any finite width of the involved energy levels. This equation is one of the most important criteria for the identification of domain formation in SLs. For doped, weakly coupled SLs, ΔV agrees with the average separation of two adjacent discontinuities in the I-V curve. However, due to the much more complex structure of a single period in QCLSs, the actual energy levels E_0, E_1, and E_2, which determine ΔV, are more difficult to identify, because the strong coupling between the different subbands has a rather complicated field dependence and field inhomogeneities occur within each period due to charge separation. Therefore, the voltage drop on one period, which corresponds to the resonance condition for the two energy levels, has to be calculated within a self-consistent model. According to Fig. 1, the average voltage spacing ΔV between two adjacent discontinuities is about 70 mV, which corresponds to a difference in field strengths of 15.5 kV/cm.

Figures 4(a) and 4(b) show the calculated conduction band profile, energy levels, and electron probability density for two periods of the cascade structure of sample A for an electric field of $F_1=13$ and $F_2=28$ kV/cm, respectively. The material parameters used in the calculation are described in Ref. 9 for an undoped structure. For the doped layers, we used the nominal doping density of 6.7×10^{17} cm^{-3} in the two GaAs layers and 4.5×10^{17} cm^{-3} in the two $Al_{0.33}Ga_{0.67}As$ layers. As shown in Fig. 4(a) for F_1, the ground state g (thick solid line) and the lowest injector state i_1 (dash-dotted line) are coupled due to the band bending caused by the inhomogeneous charge distribution. The positive space charge of the ionized donors is located within part of the injector, while the negative space charge of the electrons is trapped in the widest quantum well of the active region. Figure 4(b) displays the subband structure for $F_2=28$ kV/cm. For this field strength, the ground state g is resonantly coupled to the energy level i_2 (dashed line). The calculated difference between F_2 and F_1 is about 15 kV/cm, which is in excellent agreement with the experimental value of 15.5 kV/cm, confirming that the low-field domain is related to a resonance between g and i_1, while the high-field domain is due to resonant tunneling between g and i_2. Note that the electric-field strength F_1 at the low-field domain is considerably larger than the electric-field strength of the onset of domain formation in Fig. 1 of 9 kV/cm, which is

determined by the first discontinuity in the sweep up. Since the resonance conditions, in particular for the low-field domain, are affected by the field inhomogeneities within each period, the value for ΔV is expected to also depend on the carrier concentration in each period. For static electric-field domains, a sufficiently large charge density is necessary at the domain boundary, which might influence the carrier concentration within the individual periods. At the same time, the current density in each period and in both domains has to be the same due to current conservation.

Figures 5(a) and 5(b) show the calculated conduction band profile, energy levels, and electron probability density for about 1.5 periods of the cascade structure of sample B for an electric field of $F_1=20$ and $F_2=42$ kV/cm, respectively. For the doped layers, we used the nominal doping density of 5.0×10^{17} cm^{-3} in the two GaAs layers and 2.7×10^{17} cm^{-3} in the two $Al_{0.45}Ga_{0.55}As$ layers. The situation of sample B is different from sample A insofar as the experimental value for ΔV is significantly larger than the calculated value. While the calculated difference between F_2 and F_1 is only 10 kV/cm, the experimental value for ΔV corresponds to 25 kV/cm. Therefore, we have to use the difference between F_1 and an electric-field strength F_3, which corresponds to resonant tunneling between g and an even higher-energy injector state i_3. The corresponding value is about 22 kV/cm, which is comparable to the experimental result. Note that the I-V characteristic of sample B as shown in the inset of Fig. 3 exhibits a fine structure between two larger current jumps. These substructures may result from resonant tunneling between g and i_2. We assume that this rather complicated behavior of sample B is caused by an incomplete coincidence of the conditions for resonant tunneling, the continuity of the current, and the proper boundary charge between the global field domains for both field strengths, F_2 and F_3. Therefore, a quasibistable behavior for the local field-domain structure appears. The degree of the coincidence depends on the real sample structure and doping density and may vary between different samples.

V. CONCLUSION

We have shown that global electric-field domains are formed in GaAs/$Al_xGa_{1-x}As$ QCLSs for voltages below the threshold for lasing. For the low-field domain, an inhomogeneous field distribution within each period has been calculated, which affects the coupling conditions for resonant tunneling. The field strength of the low-field domain is attributed to the coupling of the ground state g in the active region with the lowest energy state i_1 of the adjacent, downstream injector. For the high-field domain, the field strength is related to resonant tunneling between g and adjacent injector states at higher energies (i_2 or i_3). Note that three conditions have to be fulfilled simultaneously for the global electric-field domain formation in QCLSs: (i) the resonant tunneling condition, which is affected by the field inhomogeneity within each period, (ii) the formation of a domain boundary with nonzero total charge that separates the low-field and high-field domains, and (iii) the continuity of the current density through the entire structure. The interplay of these three conditions may affect the value of the average spacing ΔV of the discontinuities in the I-V characteristics.

ACKNOWLEDGMENT

The authors would like to thank H. Kostial for sample processing.

*Permanent address: Department of Physics, Duke University, Box 90305, Durham, North Carolina 27708-0305.
†Electronic address: htgrahn@pdi-berlin.de

[1] C. Sirtori, F. Capasso, J. Faist, A. L. Hutchinson, D. L. Sivco, and A. Y. Cho, IEEE J. Quantum Electron. **34**, 1722 (1998).
[2] S.-C. Lee and A. Wacker, Phys. Rev. B **66**, 245314 (2002).
[3] S. L. Lu, L. Schrottke, R. Hey, H. Kostial, and H. T. Grahn, J. Appl. Phys. **97**, 024511 (2005).
[4] V. D. Jovanović, D. Indjin, N. Vukmirović, Z. Ikonić, P. Harrison, E. H. Linfield, H. Page, X. Marcadet, C. Sirtori, C. Worrall, H. E. Beere, and D. A. Ritchie, Appl. Phys. Lett. **86**, 211117 (2005).
[5] J. Ulrich, G. Strasser, and K. Unterrainer, Physica E (Amsterdam) **13**, 900 (2002).
[6] T. Ohtsuka, L. Schrottke, R. Hey, H. Kostial, and H. T. Grahn, J. Appl. Phys. **94**, 2192 (2003).
[7] L. L. Bonilla and H. T. Grahn, Rep. Prog. Phys. **68**, 577 (2005).
[8] M. Giehler, R. Hey, H. Kostial, S. Cronenberg, T. Ohtsuka, L. Schrottke, and H. T. Grahn, Appl. Phys. Lett. **82**, 671 (2003).
[9] L. Schrottke, S. L. Lu, R. Hey, M. Giehler, H. Kostial, and H. T. Grahn, J. Appl. Phys. **97**, 123104 (2005).
[10] K. Donovan, P. Harrison, and R. W. Kelsall, J. Appl. Phys. **89**, 3084 (2001).
[11] C. Sirtori, P. Kruck, S. Barbieri, P. Collot, J. Nagle, M. Beck, J. Faist, and U. Oesterle, Appl. Phys. Lett. **73**, 3486 (1998).
[12] H. Page, C. Becker, A. Robertson, G. Glastre, V. Ortiz, and C. Sirtori, Appl. Phys. Lett. **78**, 3529 (2001).
[13] K. K. Choi, B. F. Levine, R. J. Malik, J. Walker, and C. G. Bethea, Phys. Rev. B **35**, 4172 (1987).